

Controlling Extraction of Rare Earth Elements Using Functionalized Aryl-vinyl Phosphonic Acid Esters

Anastasia Kuvayskaya, Thomas J. Mallos, Iskander Douair, Christopher Chang, Ross E. Larsen, Mark P. Jensen,* and Alan Sellinger*



Cite This: <https://doi.org/10.1021/acs.inorgchem.3c01714>



Read Online

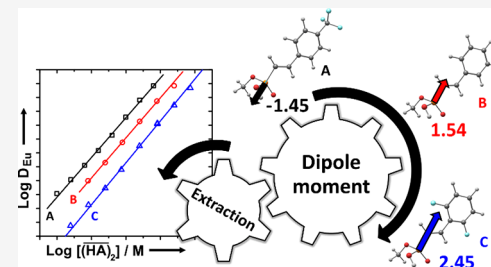
ACCESS |

Metrics & More

Article Recommendations

Supporting Information

ABSTRACT: Ligands that can discriminate between individual rare earth elements are important for production of these critical elements. A set of aryl-vinyl phosphonic acid ligands for extracting rare earth elements were designed and synthesized under the hypothesis that the strength of the rare earth–ligand interactions could be tuned by changing the dipole moment of the ligand. The ligands were synthesized via a two-step reaction procedure using a Heck coupling reaction to functionalize vinyl phosphonic acid, followed by Steglich esterification to obtain high-purity styryl phosphonic acid monoesters with varying dipole moments along the P–C bond. The metal binding strength and composition of the rare earth complexes formed with these styryl phosphonic acid monoesters were experimentally studied by liquid–liquid extraction techniques, while DFT calculations were performed to determine the dipole moments of the free and complexed ligands and the electronic structure of the complexes formed. All three prepared ligands were much stronger extracting agents for europium(III) than the dialkylphosphonic acids usually used for this separation. However, the order of increasing extraction strength was found to match the order of the decreasing calculated dipole moment along the P–C bond of the three styryl-based ligands, rather than correlating with increasing ligand basicity, as reflected by the pK_a of the ligands. These findings suggest that this approach can be used to systematically alter the extraction strength of aromatic phosphonic monoesters for rare earth element purification.



INTRODUCTION

Rare earth elements (REE) are becoming increasingly important in many high-tech industries. These strategic elements possess unique optical, magnetic, and electronic properties that make them indispensable for the glass industry, superconductors, lighting, permanent magnets, catalysis, and nuclear energy, to name a few applications.¹ The ongoing shift from fossil-based energy sources toward a green economy creates a need for a steady supply of REE. However, the state-of-the-art industrial processing of REE is costly and challenging because of the similarity in the physicochemical characteristics of these elements.

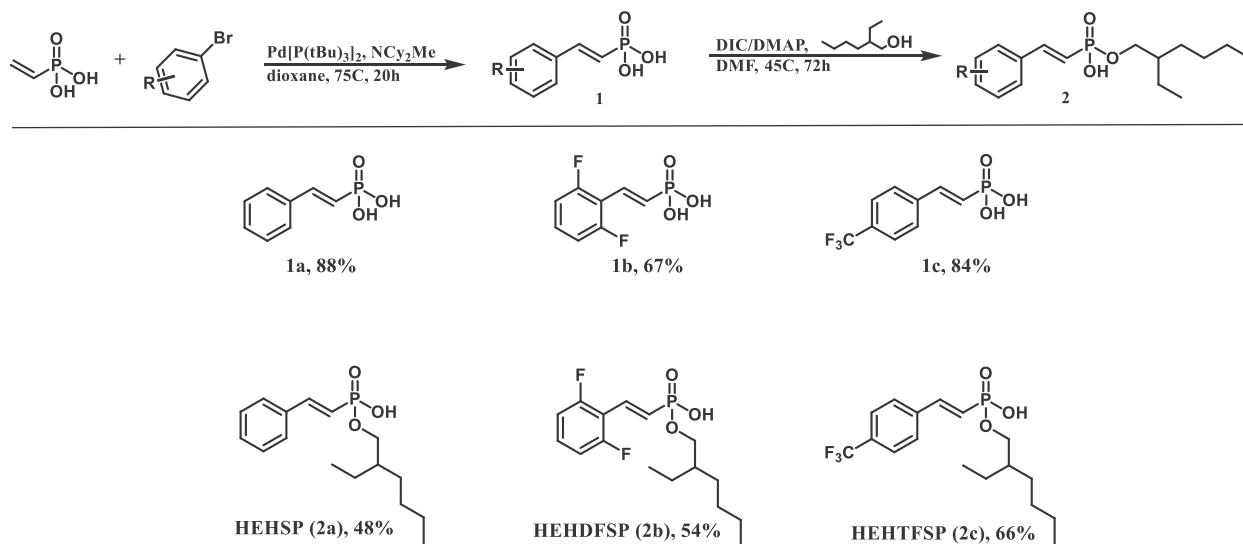
The chemical similarity of REE causes them to occur together in nature, and since different applications require particular rare earths, the naturally occurring mixtures of rare earths are currently painstakingly separated in hundreds of individual liquid–liquid extraction stages that generate significant amounts of waste at a considerable expense and environmental cost.^{2–4} Liquid–liquid extraction separations are easily deployed and readily scalable to accomplish high material throughput in continuous separation. Nevertheless, the inefficiency of current REE separations arises from the limited selectivity of the best-in-class extracting ligands such as 2-ethylhexyl phosphonic acid mono-2-ethylhexyl ester (HE-HEHP, *Supplemental Scheme S1*), di(2-ethylhexyl)phosphoric

acid (HDEHP), or bis(2,4,4-trimethylpentyl)phosphinic acid (Cyanex 272), all of which rely on the consistent, small differences in the ionic radii of adjacent REE to achieve the separation.⁵ The size selectivity of these ligands for REE arises from the particular hydrogen-bonded dimer motif of the R₂PO₂H ligands⁶ and interligand repulsion between the organic substituents of the complexed ligands, while the overall complexation strength is often correlated to the ligand basicity.^{7–12}

The economic and environmental concerns posed by the current commercially available extractants have prompted investigations into alternative REE separation approaches. Ligands that amplify or substantially alter the size selectivity for REE have been considered,^{13–15} but separation systems that can exploit other characteristics of REE for separations also have been reported, for example, separation protocols based on redox chemistry^{16–19} or magnetic fields.^{20–22} In addition to these systems, photoresponsive separations that exploit the

Received: May 25, 2023

Scheme 1. Synthetic Approach to Obtaining 2-Ethylhexyl Hydrogen Styryl Phosphonates (Top) and Obtained Ligands (Bottom)



unique electronic structure of individual REE or REE complexes have also been described.^{23–25} Recent work revealed that small changes in the conformation of coordinated ligands could tune the photophysical properties of REE complexes^{26,27} and that coordinating ligands can alter both the photophysical properties of the REE complexes and change the metals' reduction potentials.^{28,29}

Ligands that combine a systematic size selectivity with functionalities that target the electronic properties of specific REE would greatly boost the separation efficiency of rare earths. Asymmetric aryl-vinyl phosphonic acid (VPA) monoesters, such as the styryl phosphonate esters described by Huang et al.,³⁰ represent a ligand platform that could combine both strategies for REE separation. Based on the well-characterized $>\text{PO}_2\text{H}$ REE coordinating group, aryl-VPA monoester ligands also incorporate a synthetically flexible aryl-vinyl substituent attached to the phosphorus atom that provides opportunities to incorporate additional functionalities to improve the selectivity of the phosphonic acid ligands for specific REE, which would greatly simplify REE separations.

However, incorporating functionalities that improve the selectivity of the ligands for certain REE is also likely to alter the extraction strength of the ligands. Consequently, new functionalized ligand designs also need to incorporate mechanisms to keep the REE extraction strength in a range useful for separations. Prior work with aryl-vinyl substituted phosphonic acids³¹ suggests that the dipole moment of such ligands could be used to control the strength of metal–ligand interactions. In those experiments, carefully designed aryl-vinyl substituted phosphonic acids altered the electronic properties of the phosphonate-coordinated metals in several photocathode materials.^{32,33} In those instances, the change in the work function of the materials was correlated with the dipole moment of the coordinated styryl phosphonic acid ligand perpendicular to the surface.³³ The possibility of tuning the overall REE complexation strength of phosphonic acid extractants by altering the ligand dipole makes these ligands attractive candidates for next-generation separation agents because it would give a new mechanism to compensate for unwanted changes in REE extraction strength when the aryl-

vinyl substituents are coupled with redox-, magnetic-, or photoresponsive moieties.

Herein, we report modifications to the base styryl phosphonic acid mono 2-ethylhexyl ester ligand intended to alter the dipole moment of the ligand and thereby alter their REE extraction strength. The performance of three styryl phosphonic acid mono 2-ethylhexyl ester ligands as extractants for the REE europium was studied relative to the common industrial extractant HEHEHP to understand if this strategy is applicable to REE ligands. The styryl-substituted extractants form complexes similar to those of the common phosphonic acid extractants, but they are substantially stronger extractants than the dialkylphosphoric, -phosphonic, and -phosphinic acids, the extraction strength of the styryl substituted ligands for REE is better correlated to the order of the dipole moment of the coordinated ligands along the P–C bond than to ligand acidity, and manipulation of the ligand dipole offers a new design pathway for tuning the extraction strength of such ligands.

EXPERIMENTAL SECTION

Caution! $^{152,154}\text{Eu}$ is radioactive. It must be handled in properly equipped and monitored radiological facilities.

Materials. Reagents were obtained from commercial suppliers and used as received, unless otherwise indicated. Solutions of extractants were prepared by diluting known masses of extractant in chloroform ($\geq 99\%$). Aqueous solutions were prepared from 70% nitric acid and 18.2 MΩ water and standardized by titration with NaOH to the phenolphthalein end point. Radioactive $^{152,154}\text{Eu}$ was produced by neutron activation of solid Eu_2O_3 using the U.S. Geological Survey TRIGA reactor³⁴ and was then dissolved in nitric acid and found to be radiochemically pure by γ spectroscopy. Aliquots of this stock solution were evaporated to dryness and redissolved in nitric acid to prepare radiotracer solutions of $^{152,154}\text{Eu}$ for these experiments.

Ligands. Mono 2-ethylhexyl phosphonic acid 2-ethylhexyl ester (HEHEHP, 98%) was purchased from BOC Sciences and purified by the third phase method.³⁵ The styryl phosphonic acid mono 2-ethylhexyl esters were synthesized by functionalizing VPA with the appropriate aromatic moiety followed by monoesterification (Scheme 1). The addition of the aromatic moiety employed Mizoroki-Heck coupling conditions,³¹ and the subsequent alkylation used the Steglich

esterification. The specific procedures for each ligand and data on their purities can be found in the Supporting Information.

General Procedure for Synthesis of 1a–c. A Schlenk flask was charged with bromoaryl (1 equiv) and bis(*tri-tert*-butylphosphine)-palladium(0) (0.025 equiv), followed by three vacuum and N₂ refill cycles. VPA (1.2 equiv) was dissolved in anhydrous dioxane and gently bubbled with N₂ for 20 min. Anhydrous dioxane and the solution of VPA were added to the Schenk flask via a syringe with stirring. *N,N*-Dicyclohexylmethylamine (3 equiv) was added to the reaction mixture dropwise via a syringe. The reaction was heated to 80 °C for 20 h. The progress was monitored with thin layer chromatography (EtOAc/hexanes 1:4). Upon completion, the reaction mixture was cooled to room temperature. The product was extracted with EtOAc, washed three times with 5% HCl, dried over MgSO₄, and filtered. The obtained organic phase was condensed to a few mL by rotary evaporation, and the product was precipitated into dichloromethane (DCM). The filtered precipitate (white flaky crystals) was dried overnight at 45 °C under vacuum. The purity of the synthesized aryl-VPAs was verified by ¹H and ³¹P NMR.

General Procedure for Synthesis of 2a–c. A Schlenk flask was charged with styryl phosphonic acid (1 equiv) and 4-dimethylamino-pyridine (DMAP) (1 equiv), followed by three vacuum and N₂ refill cycles. DMF was added to the solution via a syringe and stirred at room temperature until solids dissolved. *N,N*'-Diisopropylcarbodiimide (DIC) (1 equiv) was then added to the solution via a syringe. 0.75 mL (1 equiv) of 2-ethylhexanol was dissolved in DMF and added to the reaction mixture dropwise. The resulting solution was heated to 40 °C for 72 h, and the progress was monitored with thin layer chromatography (EtOAc/hexanes 1:4). Upon completion, the reaction mixture was cooled to room temperature and the DMF was removed by rotary evaporation. The crude product was dissolved in DCM and placed in a freezer overnight. The precipitated 1,3-diisopropylurea byproduct was filtered out, and the DCM was removed under reduced pressure. The crude material was washed twice with hexanes, extracted with diethyl ether, and washed twice with of 10% NaOH, followed by five washes with 5% HCl. The organic phase was dried over MgSO₄ and filtered. The resulting organic phase was condensed by a rotary evaporator. The obtained product (off-white oil) was dried for 5 h at 80 °C under vacuum. FT-IR spectra of all the synthesized materials (Supplemental Figure S19) have characteristic bands of phosphonic acids: 1622 (P—O—H), 737 and 864 (C—P), 1380 (P=O) cm⁻¹. In addition, a peak at 978 cm⁻¹ was evidence of esterification and was attributed to the presence of the P—O—C bond, as discussed in the Supporting Information. The purity of the compounds obtained was verified by ¹H, ³¹P, ¹⁹F, and ¹³C NMR spectroscopy as well as potentiometric titration.

Potentiometric Titrations. All solutions for the potentiometric titrations were prepared in 75 vol % EtOH/25 vol % H₂O, and all potentiometric titrations were conducted under N₂ and thermostated at 25.0 °C. Solutions of 0.1 M NaOH were standardized by titration of dried primary standard potassium hydrogen phthalate in water to the phenolphthalein end point. Solutions of 0.01 M HCl were standardized by Gran titration with the standardized NaOH using a Mettler-Toldeo InLab semimicro combination pH electrode filled with aqueous 3 M KCl. After the standardizations were complete, the electrode was calibrated to read pcH (pcH = -log [H⁺] on the molar scale) by titration of known amounts of standardized HCl and NaOH. Dilute solutions of each ligand were prepared by dissolving measured amounts of ligand in known volumes of 75 vol % EtOH/25 vol % H₂O with or without 0.01 M HCl to give solutions of 0.009–0.017 M ligand. These solutions were titrated with standardized NaOH to determine the K_a values of each ligand. Each titration consisted of 60–70 individual pcH measurements, and the titrations of the three styryl phosphonic acid mono 2-ethylhexyl esters were conducted in duplicate. The electrode was calibrated with solutions of 75 vol % EtOH/25 vol % H₂O containing known concentrations of HCl prior to each titration, and with this procedure, the pcH readings for the ligand solutions were reproducible to ±0.007 pcH units (or ±0.4 mV). All uncertainties are reported at the 95% confidence level.

Liquid–Liquid Extraction. The stoichiometries of the extracted europium(III) complexes and the relative complexation strengths of the extractants were measured through a liquid–liquid extraction. Chloroform solutions of the ligands were contacted with equal volumes of aqueous HNO₃ solutions (0.01–0.1 M HNO₃) spiked with ^{152,154}Eu^{III} by vortexing for 5 min at 22 ± 1 °C, followed by centrifugation for 2 min. The two phases from each extraction condition were separated, and an aliquot was taken from each phase to determine the Eu content by measuring the ^{152,154}Eu γ -emission rate between 40 and 225 keV with a Packard Cobra II γ -counter. The europium distribution ratio, D_{Eu} , was then calculated as the ratio of the total concentration of Eu in the organic phase to the total concentration of Eu in the aqueous phase, $D_{\text{Eu}} = \overline{[\text{Eu}]} / [\text{Eu}]$, where the overbar indicates species in the organic phase. The uncertainty in the distribution ratios was calculated from the uncertainties in the pipetting and radioactive counting. When necessary to account for the change in activity coefficients with ionic strength, aqueous acidities were converted to the pH scale (pH = -log H⁺ activity) using the single ion activity coefficient for H⁺ calculated with the extended Debye–Hückel equation for the relevant ionic strength.

COMPUTATIONAL METHODS

To gain insight into the effect of the phosphonic acid ligand dipole moments on the Eu extraction reaction, density functional theory (DFT) calculations were performed using the Gaussian16³⁶ suite of programs and Becke's 3-parameter hybrid functional³⁷ combined with the nonlocal correlation functional provided by Perdew/Wang.³⁸ The Eu and P atoms were represented with a small-core Stuttgart-Dresden relativistic effective core potential associated with their adapted basis set.^{39–41} Additionally, the P basis set was augmented by a d-polarization function ($\alpha = 0.387$)⁴² to represent the valence orbitals. All the other atoms C, F, O, and H were described with a 6-31G (d,p), double – ζ quality basis set.^{43,44} For all ligands and complexes, geometries were optimized in two ways: in the gas phase and with polarizable continuum solvation. The desired properties were computed under the same conditions as for the optimizations (e.g., solvated optimized geometry and dipole moment from electronic structure computed with solvation). Chloroform was chosen as the solvent to mirror the experimental conditions, with solvation treated as a polarizable continuum using the default Gaussian16 self-consistent reaction field method.^{45,46} The nature of the extrema (minimum) for the ligand and ligand/RE-complex were established with analytical frequency calculations, and geometry optimizations were computed without any symmetry constraints. To gain insight into the nature and behavior of the bonds around the Eu, we performed natural bond orbital (NBO) analysis and computed the Wiberg bond index (WBI).^{47–49}

RESULTS AND DISCUSSION

Ligand Synthesis. Two synthetic routes to the target styryl phosphonic acid 2-ethylhexyl ester compounds were investigated. Complete conversion to the monoester could be achieved either by functionalizing VPA with the desired aromatic moiety followed by monoesterification or by initial alkylation of the starting material followed by the reaction with aryl bromide. Evaluation of the two approaches revealed that the first route was the more viable reaction scheme because of the ease of purifying the intermediate aryl-VPAs by precipitation from DCM and the ease of purifying the monoesters by liquid–liquid extractions.

Previously reported syntheses of styryl phosphonic acids used THF as a solvent.³⁰ However, replacing THF with dioxane increased the yields of aryl-VPAs by 5–16%. This increase could be explained by the higher boiling point of dioxane, resulting in the running reaction at an elevated temperature.

We began optimizing conditions for the monoesterification of aryl-VPAs by comparing two synthetic approaches. A microwave-assisted approach to obtaining monoalkylated phenyl, phosphinic, and phosphonic acids with catalytic addition of $[\text{bmim}][\text{BF}_4]$ ^{50,51} was utilized for esterification of VPA. The main drawback associated with this synthetic method is the use of alcohol as a reagent and a solvent, thus limiting the choices of the functionalized phosphonic acids due to solubility issues. The solubility limitations can be resolved using Steglich esterification.^{52,53} We began our optimization with the screening of three different carbodiimides: *N,N'*-dicyclohexylcarbodiimide (DCC), *N,N'*-diisopropylcarbodiimide (DIC), and *N*-(3-(dimethylamino)propyl)-*N'*-ethyl carbodiimide (EDC). Despite the ease of removal of the *N*-acyl urea byproduct when using EDC, it performed poorly regarding the conversion rate. Both DIC and DCC demonstrated high conversion rates. The DCC byproduct, *N,N*-dicyclohexylurea, is water-insoluble and partially soluble in organic solvents resulting in time- and solvent-consuming purification. *N,N'*-Diisopropylurea is more water-soluble and can be removed by solvent extraction. Consequently, we selected DIC as the most suitable carbodiimide.

We evaluated various polar solvents [dimethylformamide (DMF), acetonitrile (ACN), and tetrahydrofuran (THF)]. Traditionally, Steglich esterification is performed in DCM. Since aryl-VPAs are not soluble in DCM, only polar solvents were chosen for reaction optimization. Based on the GC-MS analysis of the reaction composition after 72 h, we selected DMF as the solvent of choice (Table 1).

Table 1. Solvent Optimization of the Steglich Esterification Reaction

entry	carbodiimide	organocatalyst	solvent	conversion ^a
1	DIC	DMAP	DMF	97%
2	DIC	DMAP	ACN	56%
3	DIC	DMAP	THF	81%

^aConversion determined by GC-MS after 72 h.

Optimization of the purification method to obtain target extractants resulted in the employment of liquid-liquid extractions with different solvent systems. After the Steglich esterifications were completed, DMF was removed under *vacuo*. The remaining crude was dissolved in DCM and left overnight in the freezer to precipitate the urea byproduct. Precipitated urea was filtered out, and DCM was removed under reduced pressure. The crude product was washed with hexanes to remove unreacted alcohol. The product was extracted with diethyl ether and washed with 10% NaOH, followed by a wash with 5% HCl.

Determination of Acid Dissociation Constants of the Ligands. The acid dissociation constants of the styryl phosphonic acid mono 2-ethylhexyl esters and HEHEHP were determined by potentiometric titration in 75 vol % EtOH/25 vol % H_2O at 25.0 °C (Supplemental Figure S20). The titration data demonstrate that HEHEHP is a weaker acid than any of the styryl phosphonic acid mono 2-ethylhexyl esters, as HEHEHP displays clear buffering action with a $\text{p}K_a$ ca. 4.3 after an initial rise in pCH as the excess HCl added to the solution was consumed at approximately 0.4 equiv of added base.

To determine the dissociation constants, the titration data were converted to buffer capacities, β ,⁵⁴

$$\beta = \frac{d[\text{Base}]}{d\text{pCH}} = \frac{c_b}{V} \frac{dV}{d\text{pCH}} \quad (1)$$

where c_b is the concentration of base added from the buret, V , is the total volume of the solution in the titration cup, and $dV/d\text{pCH}$ is the reciprocal of the derivative of the pCH vs volume titration curve. The acid dissociation constants were calculated by fitting the buffer capacities as a function of the H^+ concentration according to the general buffer capacity equation,^{54,55}

$$\beta = \ln 10 \left(\sum_i \frac{K_{a,i} c_i [\text{H}^+]}{(K_{a,i} + [\text{H}^+])^2} + [\text{H}^+] + \frac{K_w}{[\text{H}^+]} \right) \quad (2)$$

In eq 2, $K_{a,i}$ is the acid dissociation constant of species i , c_i is the total molar concentration of species i regardless of its protonation state, and K_w is the autodissociation constant of water under the solvent conditions used. K_w had been measured during the electrode calibration titrations and was determined to be $\text{p}K_w = 14.97 \pm 0.02$. The data from all the titrations of a given ligand were combined into a single data set that was fit using a simplex minimization algorithm with jackknife estimation of the uncertainty of the fitted parameters⁵⁶ to determine the ligand K_a that best reproduced the measured buffer capacities (Figure 1). The results are summarized in Table 2.

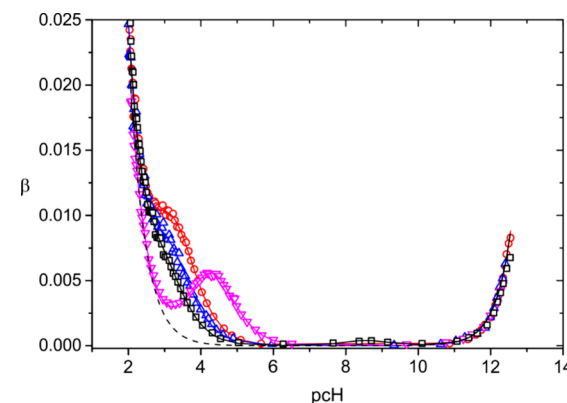


Figure 1. Fitting the buffer capacities of the ligands to determine the acid dissociation constants in 75 vol % EtOH/25 vol % H_2O at 25.0 °C. (□) HEHTFSP, (○) HEHSP, (△) HEHDFSP, (▽) HEHEHP, and (---) 0.00953 M HCl. Fits to eq 2 using the $\text{p}K_a$ values in Table 2 are indicated with solid lines.

Table 2. Acid Dissociation Constants of Phosphonic Acid Ligands in 75 vol% EtOH/25 vol% H_2O at 25.0 °C

ligand	number of points fit	$\text{p}K_a$
HEHTFSP (2c)	133	2.99 ± 0.03
HEHDFSP (2b)	120	3.13 ± 0.04
HEHSP (2a)	140	3.25 ± 0.02
HEHEHP	61	4.31 ± 0.02

The $\text{p}K_a$ measured for HEHEHP is in agreement with previously reported values determined in 75 vol % EtOH/25 vol % H_2O ($\text{p}K_a = 4.10$,⁵⁷ 4.53,⁵⁸ and 4.8⁵⁹), when the hydrogen ion activity scale used by Katzin et al.⁵⁹ is considered. Replacing the 2-ethylhexyl group attached to the phosphorus atom of HEHEHP with styryl groups increases the ligand's acidity by more than 1 order of magnitude, while

incorporation of electron-withdrawing fluorine or trifluoromethyl moieties further reduces the pK_a values compared to HEHSP. The resulting pK_a values for the styryl ligands are even lower than those of dialkylphosphoric acids such as bis(2-ethylhexyl)phosphoric acid (HDEHP, $pK_a = 3.49$ ⁵⁷) and di-n-octylphosphoric acid ($pK_a = 3.30$ ⁶⁰).

Rare Earth Extraction. The extracting strength and composition of the Eu^{3+} complexes extracted by the styryl phosphonic acid monoesters were studied by radiotracer liquid–liquid extraction experiments. The aqueous phases were composed of 0.01–0.1 M solutions of nitric acid, while the styryl phosphonic acid mono 2-ethylhexyl esters were dissolved in CHCl_3 . At the ligand concentrations studied, the phosphonic acids are expected to exist as H-bonded dimers in the CHCl_3 solutions.^{61,62} The extraction of Eu from the nitric acid solutions was studied as a function of the extractant concentration at constant aqueous acidity (Figure 2) and as a

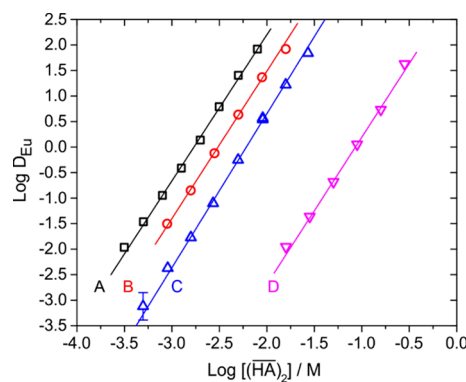


Figure 2. Extraction of Eu^{3+} by phosphonic acid ligands in CHCl_3 from 0.01005 M HNO_3 , (□) A: HEHTFSP, (○) B: HEHSP, (△) C: HEHDFSP, (▽) D: HEHEHP. Uncertainties in the distribution ratios are shown at the 95% confidence level if they are larger than the data point.

function of the aqueous acidity at a constant extractant concentration (Figure 3). The three styryl phosphonic acid monoesters are all much stronger extractants than HEHEHP, as indicated by the 1–2 order of magnitude decrease in extractant concentration required to achieve the same degree of Eu extraction (D_{Eu}) at constant acidity for HEHSP,

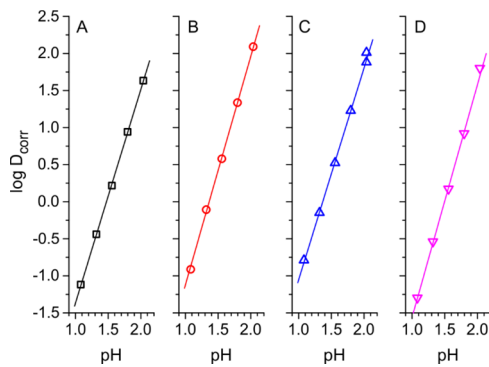
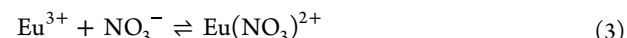


Figure 3. Extraction of Eu^{3+} by phosphonic acid ligands in CHCl_3 from HNO_3 solutions with varying acidity. (□) A: 0.0079 M (HEHTFSP)₂, (○) B: 0.016 M (HEHSP)₂, (△) C: 0.022 M (HEHDFSP)₂, (▽) D: 0.283 M (HEHEHP)₂. Uncertainties in the distribution ratios are shown at the 95% confidence level if they are larger than the data point.

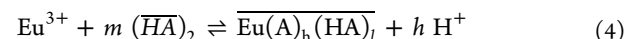
HEHDFSP, and HEHTFSP compared to HEHEHP (Figure 2). The extraction strength decreases in the order HEHTFSP > HEHSP > HEHDFSP >> HEHEHP.

While these fluoride-containing extractants have not been systematically studied before, studies of the extraction of tripositive *f*-element cations by HEHSP and other mixed alkyl/aryl organophosphorus extractants are consistent with the greater extraction strength that we observe for the styryl-substituted phosphonic acid monoesters. The extraction of La^{3+} by HEHSP dissolved in kerosene was previously observed to be stronger than that of either HEHEHP or the phosphoric acid extractant HDEHP.³⁰ Similarly, Peppard and co-workers compared HEHEHP to phenyl phosphonic acid (2-ethylhexyl) ester (HEH[PhP]) and found that HEH[PhP] outperformed HEHEHP by about 2 orders of magnitude in extracting Pm^{3+} and Cm^{3+} .⁶³ Ju and co-workers observed similar results when examining HDEHP, where they found both HEH[PhP] and its methylheptyl ester derivative extract Cm^{3+} and Cf^{3+} 2 orders of magnitude more strongly than HDEHP.⁶⁴ In another study, Peppard compared extraction by HDEHP and di[4-(1,1,3,3-tetramethylbutyl)phenyl]phosphoric acid (HDOPhP), a diaryl phosphoric acid extractant, where they found HDOPhP also outperformed HDEHP by several orders of magnitude.⁶⁵

The composition of the Eu^{3+} complexes formed with the ligands in CHCl_3 was determined by error-weighted linear regression analysis of the $\log D$ vs $\log[(\text{HA})_2]$ or pH data (Table 3), as previously described,^{66,67} with A^- representing one deprotonated phosphonic acid monoester. Under the conditions of these extractions, nitrate anions weakly compete with the phosphonic acid ligands for Eu^{3+} in the aqueous phase, with $\log K_{\text{NO}_3} = 1.22$ for Equilibrium 3 at $I = 0$ M ionic strength.⁶⁸ This aqueous nitrate complexation was accounted for in the analyses as described in the Supporting Information. The analysis of the pH dependence of $\log D$ gives slopes between 2.86 and 3.14 for all the ligands (Table 3), indicating that while nitrate does complex Eu^{3+} in the aqueous phase, the extracted complexes contain no nitrate because the electro-neutrality of both the aqueous and the organic phases is maintained by the exchange of 3 H^+ into the aqueous phase for each Eu^{3+} extracted rather than by coextraction of nitrate. Huang et al. report similar results for La^{3+} extraction by HEHSP in kerosene ($h = 3.03$).³⁰ Consequently, the general equilibria affecting the extraction are expected to be



and



where the overbar indicates species that are present in the organic phase, $2m = h + l$ is required for the mass balances of the ligand and the acidic protons, and $h = 3$ as determined from the slope of the pH dependence.

The equilibrium constants for these reactions can be combined with the metal distribution ratios, as described in the Supporting Information, to provide quantitative information on the composition of the extracted complexes. The slopes of the $\log D_{\text{Eu}}$ vs $\log[(\text{HA})_2]$ measurements give the value of m in eq 4,⁶⁷ which ranges between 2.86 and 3.01 for each of the ligands (Table 3). Our experimentally determined value of m in the HEHEHP system, 2.88 ± 0.16 , agrees well with the value found in a recent report, 2.86 ± 0.10 .⁶⁹ Our value of m for Eu^{3+} extraction by HEHSP (2.88 ± 0.09) is

Table 3. Slope Analysis of the Extraction Data Shown in Figures 2 and 3

ligand	pH	$\log D_{\text{Eu}} = m \log[(\text{HA})_2] + C_1^a$
HEHSP (2a)	2.037	$(2.88 \pm 0.09) \log[(\text{HA})_2] + (7.26 \pm 0.24)$
HEHDFSP (2b)	2.037	$(3.01 \pm 0.09) \log[(\text{HA})_2] + (6.69 \pm 0.21)$
HEHTFSP (2c)	2.037	$(2.86 \pm 0.12) \log[(\text{HA})_2] + (7.92 \pm 0.32)$
HEHEHP	2.037	$(2.88 \pm 0.16) \log[(\text{HA})_2] + (3.08 \pm 0.18)$
	$[(\text{HA})_2], \text{M}$	$\log D_{\text{Corr}} - m \log[(\text{HA})_2] = h \text{ pH} + \log K_{\text{ex}}$
HEHSP (2a)	0.016	$(3.09 \pm 0.11) \text{ pH} + (1.19 \pm 0.17)$
HEHDFSP (2b)	0.022	$(2.86 \pm 0.09) \text{ pH} + (1.08 \pm 0.14)$
HEHTFSP (2c)	0.0079	$(2.88 \pm 0.07) \text{ pH} + (2.05 \pm 0.11)$
HEHEHP	0.283	$(3.14 \pm 0.15) \text{ pH} - (3.06 \pm 0.23)$

$$^a C_1 = \log K_{\text{ex}} + h \text{ pH} + \log \gamma_{\text{Eu}^{3+}} - \log (1 + K_{\text{NO}_3} \gamma_{\text{Eu}^{3+}} \gamma_{\text{Eu}(\text{NO}_3)^{2+}}^{-1} \{\text{NO}_3^-\}).$$

consistent with the value reported for La^{3+} extraction by HEHSP from aqueous HCl into kerosene, 2.97.³⁰ Given $h = 3$ from the pH dependence and an extractant dependence of $m = 3$, mass balance requires $l = 3$. This result is commonly found for many extracting acidic organophosphorus ligands in CHCl_3 .⁶⁹ This Eu:A stoichiometry further implies that three hydrogen-bonded phosphonic acid dimers, $(\text{HA})_2$, lose a single H^+ to form a pseudo-octahedral Eu complex with three dimers (Figure 4).⁷⁰ Neither incorporation of the styryl moiety into

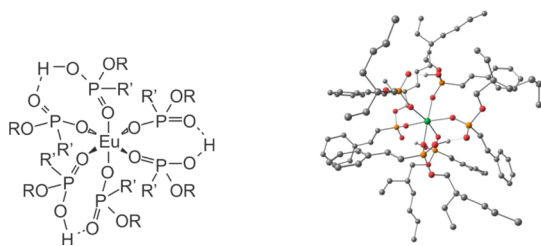


Figure 4. Schematic structure (left) of the extracted $\text{Eu}(\text{A})_3(\text{HA})_3$ complexes and the gas-phase optimized structure (right) of the Eu-HEHSP complex, with hydrogen atoms not shown. In the optimized structure, gray spheres are carbon, red spheres are oxygen, orange spheres are phosphorus, and the central green sphere is europium. See *Supplemental Tables S2–S13* for coordinates of optimized geometries of the ligands and *Supplemental Tables S14–S19* for coordinates of optimized complexes.

the extractant framework nor addition of electron-withdrawing groups to the aryl substituents alter the stoichiometry of these Eu complexes in CHCl_3 compared to HEHEHP, our reference ligand.

Computational Results. Because theoretically calculated gas phase dipole moments have been good predictors of the ability of conjugated phosphonic acids, such as the precursor aryl-VPAs 1a–1c, to modify the properties of materials when complexed to surfaces,³³ the dipole moment was calculated for the three styryl phosphonic acid mono 2-ethylhexyl ester ligands (HEHSP, HEHDFSP, and HEHTFSP), versions of these three ligands with methyl substituents replacing the 2-ethylhexyl groups (compounds 3a, 3b, and 3c; *Supplemental Scheme S1* and *Tables S2, S4, and S6*), and the reference extractant HEHEHP. The dipole moment calculations were made for both the neutral uncomplexed ligands and Eu-coordinated dimers of HEHSP, HEHDFSP, HEHTFSP, and HEHEHP in the gas phase and with implicit solvation in CHCl_3 . The methyl esters (3a–3c) were studied to speed up the initial set of dipole calculations of the free ligands. We have found previously that the electronic properties of aryl-

containing and fused-ring conjugated molecules are not appreciably changed when linear and branched alkyl chains are replaced by methyl groups.⁷¹

For *free ligands*, the dipole moment projected along the P–C bond was computed and is reported in **Table 4**. This

Table 4. Computed Dipole Moments (Debye) of Free Ligands (Projected Along P–C Bond Direction) of the Mono Methyl or 2-Ethylhexyl Esters of the Styryl Phosphonic Acids and the Ligands Complexed to Eu in $\text{EuA}_3(\text{HA})_3$ (Total Dipole Moment of Complexed Ligand), in Both the Gas Phase and in Chloroform

ligand	free ligand (P–C bond)		Eu-complexed ligand	
	gas phase	CHCl_3	gas phase	CHCl_3
HEHSP (2a)	1.68	2.12	3.40	4.35
HEHDFSP (2b)	2.61	3.34	4.54	7.05
HEHTFSP (2c)	-1.34	-1.31	2.32	2.63
HEHEHP	0.32	0.40	1.34	1.68
3a	1.54	1.68	3.13	4.09
3b	2.45	2.61	4.32	6.45
3c	-1.45	-1.34	1.98	3.49

representation of the dipole moment is approximately aligned with the length of the ligand, and it is the same metric previously used to understand surface complexation of ArVPA. It allows for direct evaluation of the impact of changing the substituents on the phosphorus atom, which, in turn, affects the properties of the oxygen atoms that coordinate the REE ions.

The calculated dipole moments of the methyl esters (3a–3c) and the 2-ethylhexyl esters (**Table 4**) follow the same order previously reported for the precursor ArVPA diacids (1a–1c).³³ While substitution of a methyl or 2-ethylhexyl group for one of the acidic hydrogens of the precursor diacid gives larger dipole moments for the monoester ligands, the change is similar across the series. Substitution of a single 2-ethylhexyl group increases the dipole moment by 0.11–0.16 D in the gas phase calculation and 0.05–0.09 D in CHCl_3 . In addition, regardless of the solvation state of the free ligands, the dipole moment vectors projected along the P–C bond direction of the new styryl extracting ligands follow the order HEHDFSP > HEHSP > HEHTFSP. The dipole moments for the free ligands projected along the P–C bond are shown in *Supplemental Figures S21–S24*. Interestingly, despite the approximate octahedral symmetry of the ligand shell around the REE metal, the magnitude of the total dipole moment of the ligands within the Eu complexes also follows this trend,

Table 5. Computed Wiberg Bond Index of the Eu–O Bonds in the $\text{EuA}_3(\text{HA})_3$ Complexes in Chloroform

ligand	Wiberg bond index					
	Eu–O1	Eu–O2	Eu–O3	Eu–O4	Eu–O5	Eu–O6
HEHSP (2a)	0.3858	0.3591	0.3768	0.3397	0.3821	0.3458
HEHDFSP (2b)	0.3594	0.3857	0.3813	0.3421	0.3488	0.3715
HEHTFSP (2c)	0.3851	0.3553	0.3739	0.3364	0.3800	0.3450
HEHEHP	0.3811	0.3540	0.3816	0.3597	0.3845	0.3510

presumably because asymmetry induced by side chains leads to a dipole moment that must be roughly proportional to the dipole moment of the individual ligands. We will see later that the ordering of the ligand dipole vector projection and the dipole moment of the complexes correlates with extraction strength.

Unlike the trend of dipole and extraction efficiency seen for the three aryl ligands, the position of HEHEHP in the order of calculated dipole moments (Table 4) is not reflective of its relative extraction ability toward rare earth elements. Replacing the conjugated vinyl aryl groups attached to the phosphonate P with a saturated 2-ethylhexyl group in HEHEHP creates a ligand with substantially different properties than the other extractants. Prior work observed that the correlation between calculated dipole moments and materials properties breaks down when aryl-VPAs are replaced with phosphonic acids bearing equivalent saturated substituents.³³ In the case of HEHEHP, substituting a 2-ethylhexyl group for the unsaturated, conjugated styryl substituents of our three new extractants creates an extractant with a low dipole moment due to the flexibility of the 2-ethylhexyl group, the lower electronegativity difference across the molecule, and a strongly diminished ability for electronic communication between the phosphonate and the P-bound substituent. In addition, HEHEHP has a much higher $\text{p}K_a$ (vide supra) and substantially different solubilities in organic solvents. Together these properties of the phosphonic acids suggest that the *dipole moments alone* of dialkylphosphonic acids such as HEHEHP will not be reliable predictors of their abilities as complexants or extracting agents but that for closely related ligands the dipole moment can be used to predict and control extraction efficiency.

While the computed dipole moments of the extracting ligands vary significantly even among the three styryl-substituted ligands, the DFT calculations reveal no significant difference in the binding strength and bond type between europium and the ligands. The calculated bond indices (Table 5) are reflective of mostly ionic interactions between the metal and each of the ligands. Furthermore, the average values of the Wiberg bond index vary by less than 1% around the mean value for the four ligands, consistent with similar degrees of electrostatically driven metal–ligand interactions across the series. This suggests that binding of the ligand to the Eu is a localized process with no substantial modification due to the overall dipole moment of the ligand. Hence, the dipole moment design of phosphonic-acid-based ligands will have little effect on complexation per se but as noted, it can alter REE complex/solvent interactions sufficiently to systematically affect extraction efficiencies.

Influence of Ligand Dipoles on Metal Extraction. The extraction reaction expressed by Equilibrium 4 describes the overall reaction between the metal cation and protonated ligand dimers in terms of the predominant species in the two phases. It is very useful for understanding the chemical species

present at equilibrium and modeling the extraction efficiency of many acidic organophosphorus extractants. However, breaking this overall equilibrium into a thermodynamic cycle of descriptive subreactions brings deeper insight into the processes and energetics involved in rare earth-ligand extraction reactions. As suggested in Figure 5, Equilibrium 4

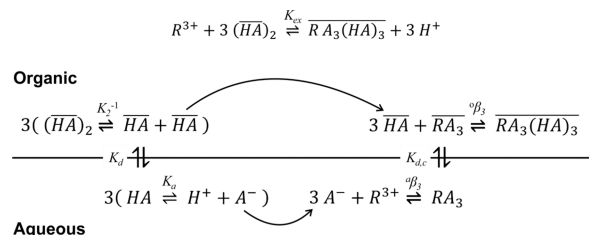
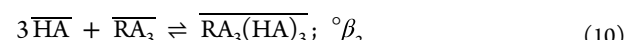


Figure 5. Thermodynamic cycle for extraction of trivalent rare earth cations, R^{3+} , by phosphonic acid monoester ligands.

for a rare earth ion, R^{3+} , can be decomposed into six subreactions, each with its own equilibrium constant,⁷²



In order to obtain Equilibrium 4 by summing Equilibria 5–10, Equilibria 5, 6, and 7 each must be multiplied by 3, so the resulting equilibrium constants will each be cubed, giving K_2^{-3} , K_d^{-3} , and K_a^3 . Then, the resulting expression for the overall extraction equilibrium constant, K_{ex} , is

$$K_{\text{ex}} = \left(\frac{K_a}{K_2} \right)^3 \left(\frac{K_{d,c}}{K_d^3} \right) ({}^a\beta_3 {}^o\beta_3) \quad (11)$$

Values of K_{ex} for each extractant are readily calculated from the pH dependence of the europium distribution ratios (Table 3). As expected from the extraction data (Figure 2), the styryl phosphonic acid monoesters show similar K_{ex} values, while K_{ex} for the reference dialkyl phosphonic acid, HEHEHP, is 4–5 orders of magnitude smaller.

While the final complexes formed in CHCl_3 are the same for all four ligands studied, the three styryl phosphonic acid ligands extract Eu more strongly than HEHEHP, the dialkyl phosphonic acid most commonly used to separate rare earths. The relative ability of similar ligands to extract rare earth cations from acidic solutions by exchanging H^+ for R^{3+} is often

attributed to differences in the acidity of the ligands, whereby more acidic ligands extract metal cations more strongly.⁷³ This is understood to result from a more favorable competition between the metal cation and protons for the more acidic ligand in the overall reaction (eq 4), since the ligand starts the reaction as a neutral, protonated species in the low dielectric constant organic phase. A more acidic ligand favors the production of A^- in the deprotonation equilibrium, giving more A^- for the rare earth to react with. Our results follow this general trend, for the styryl phosphonic ligands are substantially more acidic than HEHEHP (Table 2) and they achieve the same degree of Eu extraction at much lower ligand concentrations than HEHEHP (Figure 2 and Table 3). There is one important deviation from this trend for the Eu extraction strengths. The extraction strengths of the styryl derivative, HEHSP, and the difluoro-styryl derivative, HEHDFSP, as represented by their K_{ex} values, are reversed compared to the acidity. HEHSP, with a pK_a of 3.25, is a stronger extractant than HEHDFSP, which has a pK_a of 3.13. The opposite of the observed trend would be expected based on the usual correlation between pK_a and extraction strength.

Our selection of these styryl phosphonic acid monoester ligands as targets for new extraction reagents was not, however, based on systematic variations in the ligand acidity. Rather, the particular styryl phosphonic acid monoesters were selected based on the ability of the parent diacid aryl-VPAs (1a–1c) to systematically alter the properties of conducting oxides when coordinated to the surface of materials such as zinc oxide and indium tin oxide.³³ The key ligand parameter influencing the ability of the ligand to alter surface work functions was the dipole moment of the ligand along the P–C bond. When the experimental extraction strengths of three styryl-based ligands are compared to the gas phase dipole moments of the ligands, or any of the other calculated dipole moments in Table 4, the anomalous reversal observed in the extraction strength vs pK_a (Figure 6) instead follows the order of decreasing dipole

ligands, we observe that the order of *increasing* Eu extraction strength, HEHDFSP < HEHSP < HEHTFSP, matches the order of *decreasing* calculated dipole moment, both with the complexed ligand dipole moment and the projected dipole moment for the free ligands.

Substantial insight into the contributions of pK_a and the dipole moment to the extraction of rare earth elements by these ligands can be gained by examining the extraction cycle suggested by eq 11. Each of the three groups of terms in eq 11 represents a different aspect of the extraction process. First, the ratio K_a/K_2 considers the competition between acid dissociation and ligand dimerization through hydrogen bonding. This term represents chemical reactions intrinsic to the ligand alone. Both of the equilibrium constants in this term are expected to be strongly dependent on the polarity of the O–H bond in the ligand, and it is generally observed for acidic organophosphorus extractants that the magnitude of K_2 increases as K_a increases.^{61,62} The polarity of the O–H bond will be strongly influenced by the adjacent phosphorus atom and the properties of its aryl-vinyl substituents, which are related to the dipole moment along the P–C bond. Given the substantial differences in the pK_a values between HEHEHP and the styryl-bearing ligands, this term is particularly important in understanding the much lower value of K_{ex} observed for HEHEHP.

Second, the ratio $K_{d,c}/K^3$ describes the relative solubilities of the protonated monomeric ligand and the neutral LnA_3 complex in the two phases, which is principally determined by the physicochemical properties of the ligand and the solvents. Ligand polarity, as reflected in the overall dipole moment, certainly plays a role in determining the relative values of these equilibrium constants, but specific intermolecular solute–solvent interactions as well as general properties, such as the free energy of solvent cavitation, will also affect the importance of this term in determining the relative selectivity of extractants. Of the three groups of terms in eq 11, this term is expected to be influenced more by the changes in the overall free ligand dipole (Table S1) caused by substitution of the styryl moieties than the dipole moment along the P–C bond in the monoester ligands.

The third term, $\beta_3^0\beta_3^0$, represents the affinity of the deprotonated ligand dimer, HA_2^- , for the rare earth cation. Since the metal–ligand bonding in these complexes is predominantly electrostatic in nature, the magnitude of the negative charge on the phosphonate oxygens is key. Increasing this negative charge on the oxygens will increase the electrostatic bond strength between the metal cation and the deprotonated ligand. As is the case for the first term, variations in the partial negative charge on the oxygen will be more closely related to the dipole moment along the P–C bond than to the dipole moment of the whole ligand. However, the effect that increasing the negative charge on the oxygens will have on the dipole moment of the ligand will depend on the magnitude and direction of the dipole moment of the ligand framework. When the dipole moment vector is directed away from the oxygen, increasing the negative charge on the oxygens will decrease the magnitude of the dipole moment. This is the case for the styryl phosphonic acid monoester ligands.

CONCLUSIONS

Styryl phosphonic acid monoesters represent a promising class of extracting ligands for rare earth elements. For the three

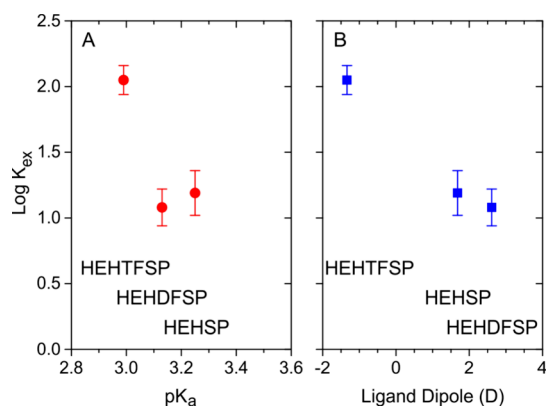


Figure 6. Correlation of Eu^{3+} extraction strength of the styryl phosphonic acid mono 2-ethylhexyl ester ligands with (A) ligand pK_a and (B) dipole moment of the neutral ligand.

moment for the three styryl phosphonic acid monoesters. On the other hand, the extraction strength of HEHEHP, which completely lacks styryl substituents and features only saturated 2-ethylhexyl groups and relatively symmetric alkylation of the phosphonate, does not follow the trend in dipole moments. Nevertheless, this was expected from the earlier studies of surface functionalization, where only ArVPA ligands followed the dipole moment correlation.³³ For the styryl-substituted

ligands developed here, incorporating an aryl-vinyl moiety into a phosphonic acid mono 2-ethylhexyl framework lowers the pK_a of the ligand and greatly increases the extraction strength of the phosphonic acid, but it does so without altering the extraction equilibria or the stoichiometry of the extracted complexes. This suggests that this class of extracting ligands can provide a platform for further tuning the K_{ex} or other properties of the extracted complexes by varying the aryl substituent. Such alterations might be used to improve the intralanthanide selectivity of the extraction while maintaining the K_{ex} values within an ideal window for a given separation or impart particular photophysical or electrochemical properties to the complexes.

In addition, the utility of the gas phase dipole moment for describing the surface chemistry of ArVPA ligands, first described by Koldemir et al.,³³ also extends to describing the extraction strength of the aryl-VPA mono 2-ethylhexyl esters for Eu^{3+} . The observation of a correlation between extraction efficiency and the dipole moment of isolated ligands may be useful for computational ligand design within families of molecules because the dipole of a single ligand can be calculated with much less computational expense than is needed for a full complex. Moreover, the computational expense of calculations with flexible 2-ethylhexyl groups appears unnecessary because the methyl esters display dipoles similar to those of the longer chain branched alkyl substituents. Although the ligand dipole moment can affect all of the key equilibria that affect metal extraction, within the series of aryl-vinyl ligands we studied, the ligand dipole moment appears particularly important in determining the relative solubilities of the protonated extractant and neutral metal complex in the two phases and also in determining the overall affinity of HA_2^- , the singly deprotonated ligand dimer, for a given metal cation. As such, the gas phase dipole moments of aryl-VPA monoesters should be considered as a useful supplement to the free energy correlation between $\log K_{ex}$ and pK_a for understanding the extraction strength of these compounds.

ASSOCIATED CONTENT

Supporting Information

The Supporting Information is available free of charge at <https://pubs.acs.org/doi/10.1021/acs.inorgchem.3c01714>.

Structural diagrams of ligands; experimental methods and details of synthetic procedures; ^1H , ^{31}P , ^{13}C , and ^{19}F NMR, UV-vis, and FT-IR spectra of ligands; potentiometric titration data for each ligand; details of equilibrium analysis of the solvent extraction data; summaries of calculated ligand dipoles; and coordinates of optimized ligand geometries ([PDF](#))

AUTHOR INFORMATION

Corresponding Authors

Mark P. Jensen — Department of Chemistry and Nuclear Science and Engineering Program, Colorado School of Mines, Golden, Colorado 80401, United States;  orcid.org/0000-0003-4494-6693; Email: mjensen@mines.edu

Alan Sellinger — Department of Chemistry and Materials Science Program, Colorado School of Mines, Golden, Colorado 80401, United States; National Renewable Energy Laboratory, Golden, Colorado 80401, United States;  orcid.org/0000-0001-6705-1548; Email: aselli@mines.edu

Authors

Anastasia Kuvayskaya — Department of Chemistry, Colorado School of Mines, Golden, Colorado 80401, United States;  orcid.org/0009-0007-8135-7106

Thomas J. Mallos — Department of Chemistry, Colorado School of Mines, Golden, Colorado 80401, United States

Iskander Douair — National Renewable Energy Laboratory, Golden, Colorado 80401, United States

Christopher Chang — National Renewable Energy Laboratory, Golden, Colorado 80401, United States;  orcid.org/0000-0003-3800-6021

Ross E. Larsen — National Renewable Energy Laboratory, Golden, Colorado 80401, United States; Renewable and Sustainable Energy Institute, University of Colorado Boulder, Boulder, Colorado 80309, United States;  orcid.org/0000-0002-2928-9835

Complete contact information is available at:

<https://pubs.acs.org/10.1021/acs.inorgchem.3c01714>

Notes

The authors declare no competing financial interest.

ACKNOWLEDGMENTS

This work was authored in part by the National Renewable Energy Laboratory (NREL), operated by Alliance for Sustainable Energy, LLC, for the U.S. Department of Energy (DOE) under Contract No. DE-AC36-08GO28308. This work was funded by the Separation Science Program, Division of Chemical Sciences, Geosciences, and Biosciences (CSGB) Division, and the Physical Behavior of Materials Program, Materials Sciences and Engineering (MSE) Division, within the Office of Basic Energy Sciences, Office of Science, DOE through the Materials and Chemical Sciences Research on Critical Materials National Laboratory Program (LAB 20-2034). A.K. also acknowledges the Department of Chemistry at Colorado School of Mines for providing funding through teaching assistantships. T.J.M. was partly supported by the U.S. Department of Energy Offices of Nuclear Energy and Environmental Management under the Radiochemistry Traineeship Program, DE-NE0008582. The views expressed in the article do not necessarily represent the views of the DOE or the U.S. Government. The U.S. Government retains and the publisher, by accepting the article for publication, acknowledges that the U.S. Government retains a nonexclusive, paid-up, irrevocable, worldwide license to publish or reproduce the published form of this work, or allow others to do so, for U.S. Government purposes.

REFERENCES

- (1) Binnemans, K.; Jones, P. T.; Blanpain, B.; Van Gerven, T.; Yang, Y.; Walton, A.; Buchert, M. Recycling of Rare Earths: A Critical Review. *J. Cleaner Prod.* **2013**, *51*, 1–22.
- (2) Arshi, P. S.; Vahidi, E.; Zhao, F. Behind the Scenes of Clean Energy: The Environmental Footprint of Rare Earth Products. *ACS Sustainable Chem. Eng.* **2018**, *6*, 3311–3320.
- (3) Lee, J. C. K.; Wen, Z. Pathways for Greening the Supply of Rare Earth Elements in China. *Nat. Sustainable* **2018**, *1*, 598–605.
- (4) Xie, F.; Zhang, T. A.; Dreisinger, D.; Doyle, F. A Critical Review on Solvent Extraction of Rare Earths from Aqueous Solutions. *Miner. Eng.* **2014**, *56*, 10–28.
- (5) Nash, K. L.; Jensen, M. P. Analytical-scale Separations of the Lanthanides: A Review of Techniques and Fundamentals. *Sep. Sci. Technol.* **2001**, *36*, 1257–1282.

(6) Ferraro, J. R.; Peppard, D. F. Structural Aspects of Organophosphorus Extractants and Their Metallic Complexes as Deduced from Spectral and Molecular Weight Studies. *Nucl. Sci. Eng.* **1963**, *16*, 389–400.

(7) Weaver, B.; Shoun, R. R. Comparison of Some Monoacidic Organophosphorus Esters as Lanthanide-Actinide Extractors and Separators. *J. Inorg. Nucl. Chem.* **1971**, *33*, 1909–1917.

(8) Sella, C.; Nortier, P.; Bauer, D. A Molecular Modelling Study about the Influence of the Structure of Alkyl Chains of Dialkyl Phosphoric Acids on Liquid-Liquid Lanthanide(III) Extraction. *Solvent Extr. Ion Exch.* **1997**, *15*, 931–960.

(9) Comba, P.; Gloe, K.; Inoue, K.; Krüger, T.; Stephan, H.; Yoshizuka, K. Molecular Mechanics Calculations and the Metal Ion Selective Extraction of Lanthanoids. *Inorg. Chem.* **1998**, *37*, 3310–3315.

(10) Takahashi, T.; Nishizawa, H.; Tsuchiya, Y.; Sato, T. Effect of Changes in Structure of Phosphoric Acid Esters on Extractability of Rare Earths: Extraction of Rare Earths by Phosphoric Acid Esters Containing Bulk Alkyl Groups I. *Sigen-to-Sozai* **1995**, *111*, 109–113.

(11) Ishida, K.; Takeda, S.; Takahashi, T.; Sato, T. Effect of Changes in Structure of Phosphoric Acid Esters on Extractability of Rare Earths: Extraction of Rare Earths by Phosphoric Acid Esters Containing Bulk Alkyl Groups II. *Sigen-to-Sozai* **1995**, *111*, 114–118.

(12) Hino, A.; Hirai, T.; Komasawa, I. Acidic Phosphinates with Different Alkyl Groups as Extractants for Rare Earths. *J. Chem. Eng. Jpn.* **1996**, *29*, 1041–1044.

(13) Jensen, M. P.; Chiarizia, R.; Ulicki, J. S.; Spindler, B. D.; Murphy, D. J.; Hossain, M.; Roca-Sabio, A.; de Blas, A.; Rodríguez-Blas, T. Solvent Extraction Separation of Trivalent Americium from Curium and the Lanthanides. *Solvent Extr. Ion Exch.* **2015**, *33*, 329–345.

(14) Cole, B. E.; Falcones, I. B.; Cheisson, T.; Manor, B. C.; Carroll, P. J.; Schelter, E. J. A Molecular Basis to Rare Earth Separations for Recycling: Tuning the TriNO_x Ligand Properties for Improved Performance. *Chem. Commun.* **2018**, *54*, 10276–10279.

(15) Hu, A.; MacMillan, S. N.; Wilson, J. J. Macrocyclic Ligands with an Unprecedented Size-Selectivity Pattern for the Lanthanide Ions. *J. Am. Chem. Soc.* **2020**, *142*, 13500–13506.

(16) Peppard, D. F.; Horwitz, E. P.; Mason, G. W. Comparative Liquid-Liquid Extraction Behaviour of Europium (II) and Europium (III). *J. Inorg. Nucl. Chem.* **1962**, *24*, 429–439.

(17) Nishihama, S.; Hirai, T.; Komasawa, I. Advanced Liquid-Liquid Extraction Systems for the Separation of Rare Earth Ions by Combination of Conversion of the Metal Species with Chemical Reaction. *J. Solid State Chem.* **2003**, *171*, 101–108.

(18) Fang, H.; Cole, B. E.; Qiao, Y.; Bogart, J. A.; Cheisson, T.; Manor, B. C.; Carroll, P. J.; Schelter, E. J. Electro-kinetic Separation of Rare Earth Elements Using a Redox-Active Ligand. *Angew. Chem., Int. Ed.* **2017**, *56*, 13450–13454.

(19) Cole, B. E.; Cheisson, T.; Higgins, R. F.; Nakamaru-Ogiso, E.; Manor, B. C.; Carroll, P. J.; Schelter, E. J. Redox-Driven Chelation and Kinetic Separation of Select Rare Earths Using a Tripodal Nitroxide Proligand. *Inorg. Chem.* **2020**, *59*, 172–178.

(20) Higgins, R. F.; Cheisson, T.; Cole, B. E.; Manor, B. C.; Carroll, P. J.; Schelter, E. J. Magnetic Field Directed Rare-Earth Separations. *Angew. Chem., Int. Ed.* **2020**, *59*, 1851–1856.

(21) Fan, B.; Li, F.; Cheng, Y.; Wang, Z.; Zhang, N.; Wu, Q.; Bai, L.; Zhang, X. Rare-Earth Separations Enhanced by Magnetic Field. *Sep. Purif. Technol.* **2022**, *301*, No. 122025.

(22) Franczak, A.; Binnemans, K.; Fransaer, J. Magnetomigration of Rare-Earth Ions in Inhomogeneous Magnetic Fields. *Phys. Chem. Chem. Phys.* **2016**, *18*, 27342–27350.

(23) Donohue, T. Photochemical Separation of Europium from Lanthanide Mixtures in Aqueous Solution. *J. Chem. Phys.* **1977**, *67*, 5402–5404.

(24) Donohue, T. Lanthanide Photochemistry Initiated in f-f Transitions. *J. Am. Chem. Soc.* **1978**, *100*, 7411–7413.

(25) Donohue, T. Photochemical Separation of Cerium from Rare Earth Mixtures in Aqueous Solution. *Chem. Phys. Lett.* **1979**, *61*, 601–604.

(26) Bogart, J. A.; Cole, B. E.; Boreen, M. A.; Lippincott, C. A.; Manor, B. C.; Carroll, P. J.; Schelter, E. J. Accomplishing Simple, Solubility-based Separations of Rare Earth Elements with Complexes Bearing Size-Sensitive Molecular Apertures. *Proc. Natl. Acad. Sci. U. S. A.* **2016**, *113*, 14887–14892.

(27) Cheisson, T.; Cole, B. E.; Manor, B. C.; Carroll, P. J.; Schelter, E. J. Phosphoryl-Ligand Adducts of Rare Earth-TriNO_x Complexes: Systematic Studies and Implications for Separations Chemistry. *ACS Sustainable Chem. Eng.* **2019**, *7*, 4993–5001.

(28) Liu, G. K.; Jensen, M. P.; Almond, P. M. Systematic Behavior of Charge-Transfer Transitions and Energy Level Variation in Soft Donor Complexes of the Trivalent Lanthanides. *J. Phys. Chem. A* **2006**, *110*, 2081–2088.

(29) Qiao, Y.; Schelter, E. J. Lanthanide Photocatalysis. *Acc. Chem. Res.* **2018**, *51*, 2926–2936.

(30) Huang, K.; Jia, Y.; Wang, S.; Yang, J.; Zhong, H. A Novel Method for Synthesis of Styryl Phosphonate Monoester and its Application in La(III) Extraction. *J. Rare Earths* **2020**, *38*, 649–656.

(31) McNichols, B. W.; Koubek, J. T.; Sellinger, A. Single-step Synthesis of Styryl Phosphonic Acids via Palladium-catalyzed Heck Coupling of Vinyl Phosphonic Acid with Aryl Halides. *Chem. Commun.* **2017**, *53*, 12454–12456.

(32) MacLeod, B. A.; Steirer, K. X.; Young, J. L.; Koldemir, U.; Sellinger, A.; Turner, J. A.; Deutsch, T. G.; Olson, D. C. Phosphonic Acid Modification of GaInP₂ Photocathodes Toward Unbiased Photoelectrochemical Water Splitting. *ACS Appl. Mater. Interfaces* **2015**, *7*, 11346–11350.

(33) Koldemir, U.; Braid, J. L.; Morgenstern, A.; Eberhart, M.; Collins, R. T.; Olson, D. C.; Sellinger, A. Molecular Design for Tuning Work Functions of Transparent Conducting Electrodes. *J. Phys. Chem. Lett.* **2015**, *6*, 2269–2276.

(34) Koehl, M. A.; Rundberg, R. S.; Shafer, J. C. Relative Fission Product Yields in the USGS TRIGA MARK I Reactor. *J. Radioanal. Nucl. Chem.* **2017**, *314*, 1375–1381.

(35) Zhengshui, H.; Ying, P.; Wanwu, M.; Xun, F. Purification of Organophosphorus Acid Extractants. *Solvent Extr. Ion Exch.* **1995**, *13*, 965–976.

(36) Frisch, M. J.; Trucks, G. W.; Schlegel, H. B.; Scuseria, G. E.; Robb, M. A.; Cheeseman, J. R.; Scalmani, G.; Barone, V.; Petersson, G. A.; Nakatsuji, H.; Li, X.; Caricato, M.; Marenich, A. V.; Bloino, J.; Janesko, B. G.; Gomperts, R.; Mennucci, B.; Hratchian, H. P.; Ortiz, J. V.; Izmaylov, A. F.; Sonnenberg, J. L.; Williams, D.; Ding, F.; Lipparini, F.; Egidi, F.; Goings, J.; Peng, B.; Petrone, A.; Henderson, T.; Ranasinghe, D.; Zakrzewski, V. G.; Gao, J.; Rega, N.; Zheng, G.; Liang, W.; Hada, M.; Ehara, M.; Toyota, K.; Fukuda, R.; Hasegawa, J.; Ishida, M.; Nakajima, T.; Honda, Y.; Kitao, O.; Nakai, H.; Vreven, T.; Throssell, K.; Montgomery, Jr., J. A.; Peralta, J. E.; Ogliaro, F.; Bearpark, M. J.; Heyd, J. J.; Brothers, E. N.; Kudin, K. N.; Staroverov, V. N.; Keith, T. A.; Kobayashi, R.; Normand, J.; Raghavachari, K.; Rendell, A. P.; Burant, J. C.; Iyengar, S. S.; Tomasi, J.; Cossi, M.; Millam, J. M.; Klene, M.; Adamo, C.; Cammi, R.; Ochterski, J. W.; Martin, R. L.; Morokuma, K.; Farkas, O.; Foresman, J. B.; Fox, D. J. *Gaussian 16 Rev. C.01*; Gaussian Inc.: Wallingford, CT, 2016.

(37) Burke, K.; Perdew, J. P.; Wang, Y. Derivation of a Generalized Gradient Approximation: The PW91 Density Functional. In *Electronic Density Functional Theory: Recent Progress and New Directions*, Dobson, J. F.; Vignale, G.; Das, M. P., Eds. Plenum: New York, 1998; pp 81–112.

(38) Becke, A. D. Density-Functional Thermochemistry. III. The Role of Exact Exchange. *J. Chem. Phys.* **1993**, *98*, 5648–5652.

(39) Cao, X.; Dolg, M. Segmented Contraction Scheme for Small-Core Actinide Pseudopotential Basis Sets. *J. Mol. Struct.: THEOCHEM* **2004**, *673*, 203–209.

(40) Cao, X.; Dolg, M.; Stoll, H. Valence Basis Sets for Relativistic Energy-Consistent Small-Core Actinide Pseudopotentials. *J. Chem. Phys.* **2003**, *118*, 487–496.

(41) Küchle, W.; Dolg, M.; Stoll, H.; Preuss, H. Energy-Adjusted Pseudopotentials for the Actinides. Parameter Sets and Test Calculations for Thorium and Thorium Mmonoxide. *J. Chem. Phys.* **1994**, *100*, 7535–7542.

(42) Höllwarth, A.; Böhme, M.; Dapprich, S.; Ehlers, A. W.; Gobbi, A.; Jonas, V.; Köhler, K. F.; Stegmann, R.; Veldkamp, A.; Frenking, G. A Set of d-Polarization Functions for Pseudo-Potential Basis Sets of the Main Group Elements Al–Bi and f-type Polarization Functions for Zn, Cd Hg. *Chem. Phys. Lett.* **1993**, *208*, 237–240.

(43) McLean, A. D.; Chandler, G. S. Contracted Gaussian Basis Sets for Molecular Calculations. I. Second Row Atoms, Z = 11–18. *J. Chem. Phys.* **1980**, *72*, 5639–5648.

(44) Hehre, W. J.; Ditchfield, R.; Pople, J. A. Self—Consistent Molecular Orbital Methods. XII. Further Extensions of Gaussian—Type Basis Sets for Use in Molecular Orbital Studies of Organic Molecules. *J. Chem. Phys.* **1972**, *56*, 2257–2261.

(45) Cossi, M.; Rega, N.; Scalmani, G.; Barone, V. Energies, Structures, and Electronic Properties of Molecules in Solution with the C-PCM Solvation Model. *J. Comput. Chem.* **2003**, *24*, 669–681.

(46) Barone, V.; Cossi, M. Quantum Calculation of Molecular Energies and Energy Gradients in Solution by a Conductor Solvent Model. *J. Phys. Chem. A* **1998**, *102*, 1995–2001.

(47) Reed, A. E.; Weinhold, F. Natural Localized Molecular Orbitals. *J. Chem. Phys.* **1985**, *83*, 1736–1740.

(48) Reed, A. E.; Weinstock, R. B.; Weinhold, F. Natural Population Analysis. *J. Chem. Phys.* **1985**, *83*, 735–746.

(49) Weinhold, F.; Foster, J. Natural Hybrid Orbitals. *J. Am. Chem. Soc.* **1980**, *102*, 7211–7218.

(50) Henyecz, R.; Kiss, A.; Morocz, V.; Kiss, N. Z.; Keglevich, G. Synthesis of Phosphonates from Phenylphosphonic Acid and its Monoesters. *Synth. Commun.* **2019**, *49*, 2642–2650.

(51) Kiss, N. Z.; Keglevich, G. Microwave-assisted direct esterification of cyclic phosphinic acids in the presence of ionic liquids. *Tetrahedron Lett.* **2016**, *57*, 971–974.

(52) Molnár, K.; Behra, J.; Takács, L.; Kádár, M.; Kardos, Z.; Faigl, F. A Convenient Procedure for the Synthesis of 2,2,2-Trifluoroethyl Methyl 2-Oxoalkylphosphonates. *Phosphorus, Sulfur, Silicon Relat. Elem.* **2015**, *190*, 677–680.

(53) Xiong, B.; Wang, G.; Zhou, C.; Liu, Y.; Li, J.; Zhang, P.; Tang, K. DCC-Assisted Direct Esterification of Phosphinic and Phosphoric Acids with O-nucleophiles. *Phosphorus, Sulfur, and Silicon Relat. Elem.* **2018**, *193*, 239–244.

(54) Van Slyke, D. D. On the Meseurement of Buffer Values and on the Relationship of Buffer Value to the Dissociation Constant of the Buffer and the Concentration and Reaction of the Buffer Solution. *J. Biol. Chem.* **1922**, *52*, 525–570.

(55) Kilpi, S. A Differential Potentiometric Method of Measuring Acid and Base Dissociation Constants. *J. Am. Chem. Soc.* **1952**, *74*, 5296–5298.

(56) Caceci, M. S. Estimating Error Limits in Parametric Curve Fitting. *Anal. Chem.* **1989**, *61*, 2324–2327.

(57) Cox, M.; Elizalde, M.; Castresana, J.; Miralles, N. *Interfacial Properties and Metal Extraction Chemistry of the Organophosphorus Acids: $(RO)_2PO(OH)$; $(RO)RPO(OH)$; $R_2PO(OH)$* . In Proceedings of the International Solvent Extraction Conference 1983; Denver: Colorado, 1983; pp 268–269.

(58) Binghua, Y.; Nagaosa, Y.; Satake, M.; Nomura, A.; Horita, K. Solvent Extraction of Metal Ions and Separation of Nickel(II) from other Metal Ions by Organophosphorus Acids. *Solvent Extr. Ion Exch.* **1996**, *14*, 849–870.

(59) Katzin, L. I.; Mason, G. W.; Peppard, D. F. Infrared Spectral Observation on the P = O Group Vibration of Some Homogeneous Series of Organic Derivatives of P(V). *Spectrochim. Acta, Part A* **1978**, *34*, 57–61.

(60) Vandegrift, G. F.; Horwitz, E. P. Interfacial Activity of Liquid–liquid Extraction Reagents. I. Dialkyl Phosphorous Based Acids. *J. Inorg. Nucl. Chem.* **1980**, *42*, 119–125.

(61) Marcus, Y. *Equilibrium Constants of Liquid-Liquid Distribution Reactions: Organophosphorus Extractants*; Butterworth, 1974.

(62) Kolarik, Z. Review: Dissociation, Self-Association, and Partition of Monoacidic Organophosphorus Extractants. *Solvent Extr. Ion Exch.* **2010**, *28*, 707–763.

(63) Peppard, D. F.; Mason, G. W.; Hucher, I. Acidic Esters of Phosphoric Acid as Selective Extractants for Metallic Cations – Selected M(III) Tracer Studies. *J. Inorg. Nucl. Chem.* **1961**, *18*, 245–258.

(64) Ju, C.; Wang, R.; Fan, Z. The Extraction of Californium and Curium with some Mono-Acidic Organophosphorus Esters. *He Huaxue Yu Fangshe Huaxue* **1982**, 186–190.

(65) Peppard, D. F.; Mason, G. W.; Driscoll, W. J.; Sironen, R. J. Acidic Esters of Orthophosphoric Acid as Selective Extractants for Metallic Cations—Tracer Studies. *J. Inorg. Nucl. Chem.* **1958**, *7*, 276–285.

(66) Picayo, G. A.; Etz, B. D.; Vyas, S.; Jensen, M. P. Characterization of the ALSEP Process at Equilibrium: Speciation and Stoichiometry of the Extracted Complex. *ACS Omega* **2020**, *5*, 8076–8089.

(67) Unger, A. J.; Jensen, M. P. Discrepancies in Solvent Extraction Slope Analysis Caused by Aqueous Buffer Complexation. *Solvent Extr. Ion Exch.* **2020**, *38*, 388–400.

(68) Smith, R. M.; Martell, A. E.; Motekaitis, R. J. *Critically Selected Stability Constants of Metal Complexes Database Version 8.0*; NIST Standard Reference Data: Gaithersburg, Maryland, USA, 2004; Vol. 46.

(69) Lécrivain, T.; Kimberlin, A.; Dodd, D. E.; Miller, S.; Hobbs, I.; Campbell, E.; Heller, F.; Lapka, J.; Huber, M.; Nash, K. L. The Effect of Organic Diluent on the Extraction of Eu(III) by HEH[EHP]. *Solvent Extr. Ion Exch.* **2019**, *37*, 284–296.

(70) Cocalia, V. A.; Jensen, M. P.; Holbrey, J. D.; Spear, S. K.; Stepinski, D. C.; Rogers, R. D. Identical Extraction Behavior and Coordination of Trivalent or Hexavalent f-element Cations using Ionic Liquid and Molecular Solvents. *Dalton Trans.* **2005**, 1966–1971, DOI: [10.1039/B502016F](https://doi.org/10.1039/B502016F).

(71) Owczarczyk, Z. R.; Braunecker, W. A.; Garcia, A.; Larsen, R.; Nardes, A. M.; Kopidakis, N.; Ginley, D. S.; Olson, D. C. 5,10-Dihydroindolo[3,2-b]indole-Based Copolymers with Alternating Donor and Acceptor Moieties for Organic Photovoltaics. *Macromolecules* **2013**, *46*, 1350–1360.

(72) Kolarik, Z.; Pankova, H. Acidic Organophosphorus Extractants – I. Extraction of Lanthanides by Means of Dialkyl Phosphoric Acids – Effect of Structure and Size of Alkyl Group. *J. Inorg. Nucl. Chem.* **1966**, *28*, 2325–2333.

(73) Sekine, T.; Hasegawa, Y. *Solvent Extraction Chemistry*; Marcel Dekker: New York, 1977.